Variable Thickness Model for Fluid Films under Large Displacement

Pavel Grinfeld

Department of Mathematics, Drexel University, Philadelphia, Pennsylvania 19105, USA

(Received 7 June 2010; published 23 September 2010)

We propose dynamic nonlinear equations for free thin fluid films. The obtained numerical solutions display a number of features consistent with recent experiments with fluid films under large deformations. In particular, we observe dynamic thickening. Our analysis is based on a two-dimensional model. The film's thickness is represented by the two-dimensional density ρ. We show that a broad range of effects can be captured by a proper internal energy function $e(\rho)$.

DOI: 10.1103/PhysRevLett.105.137802 PACS numbers: 68.15.+e, 68.18.−g, 75.70.−i

Introduction.—Fluid films display an astonishing array of physical effects: static and dynamic, macroscopic and nanoscale—at times, simultaneously in a single film. Static effects go well beyond the study of minimal surfaces, as films display variations in thickness, surfactant density, and interaction with external fields [1]. Predictably, the dynamics is even richer. Fluid films display turbulence [2–5], tremendous variations in thickness [3,4,6], the Marangoni effect [7], draining and reverse draining [8], ejection of droplets [9], rupture [10], self-adaptation [11], and chaotic behavior [12].

Only a small fraction of the dynamic effects can be described by linear models which often lead to the classical wave equation solved on the equilibrium configuration [13–15]. The rest require deeply nonlinear analysis, as fluid films undergo large deformations and variations in thickness.

With respect to nonlinear oscillations, we were particularly intrigued by the experimental results of Boudaoud *et al.* [11] and Drenckhan *et al.* [9]. Both studies observed variations in thickness at large amplitudes. In [9], ejection of droplets was reported. In [11], concentration of thickness at the antinodes of oscillations was observed and a nonlinear theoretical explanation was presented. We set out to take a more general approach to modeling fluid films. We consider the general dynamic behavior of free fluid films under arbitrarily large deformations from the equilibrium configuration. Even though our model is inertial and excludes a driving mechanism, we predict variations in density consistent with experiments reported in [9,11].

In order to focus our attention on the nonlinear phenomena, we purposefully choose a simplified model. We treat the fluid film as a two-dimensional continuum S and represent its thickness by a two-dimensional density function ρ. Since the fluid is essentially incompressible in the three-dimensional sense, ρ is indeed nothing but thickness. There is strong experimental evidence [16] that this approach can capture a very broad range of effects.

We assume that the restoring force can be captured by the proper choice of the internal energy density (per unit mass) function e and in this work we assume that e is a function only of ρ, that is $e = e(\rho)$. The total potential energy V is given by $V = \int_S \rho e(\rho) dS$. The classical Laplace model for surface tension is obtained by taking

$$e(\rho) = \frac{\sigma}{\rho}, \tag{1}$$

where σ is the surface energy density per unit mass. Here, we assume that σ is uniform, but to allow surface tension gradients does not pose much of a conceptual challenge.

The assumption that e is a function only of ρ captures a wide range of effects. For example, equilibrium fluid films display the tendency to have uniform thickness. This effect can be captured by

$$e(\rho) = \frac{\sigma}{\rho} + \frac{\delta}{2}(\rho - \rho_0)^2, \tag{2}$$

where δ is a positive constant and ρ_0 is a constant that may depend on the total mass of the fluid film. The presence of a surfactant, such as soap, may essentially impose a minimum thickness. This phenomenon may be captured by an expression such as

$$e(\rho) = \frac{\sigma}{\rho} + \frac{\tau}{(\rho - \rho_{\text{minimum}})^3} \tag{3}$$

that "discourages" the film from approaching ρ_{minimum}.

A number of phenomena are excluded by the assumption that e is a function only of ρ. For example, the modeling of biological membranes must consider explicit dependence of e on the curvature tensor [17]. Liquid crystalline films require explicit dependence on the normal $\mathbf{N}$, a unit director vector field $\mathbf{l}$ and its surface gradients $\nabla\mathbf{l}$. These and other generalizations were considered in [18].

Unlike earlier publications [13,14], we allow arbitrarily large normal velocities of material particles, arbitrarily large deviations of the film from its equilibrium configuration, and arbitrarily large changes in the film's thickness. At the same time, following [13,14], we assume that tangential velocities are negligible compared to normal velocities. This assumption results in a crucial simplification of the system by reducing the number of unknowns and equations from four to two. Further, we disregard the

interaction between the fluid film and the ambient air and assume no viscous dissipation. It has been argued that viscous dissipation is negligible [16].

Proposed dynamic system.—We study a free fluid film that spans a stationary wire contour. As stated previously, we consider the case where the tangential velocities can be neglected compared to the normal velocity C. $C = 0$ at the contour boundary. We disregard viscosity and interaction with the ambient air. The fluid that makes up the film in incompressible in the three-dimensional sense. Therefore, the two-dimensional density ρ captures the thickness of the film.

We place no size restrictions on C and the rate of change in density ρ. We analyze a system of partial differential equations in which the initial configuration S is given along with the initial values for C and ρ. The proposed dynamic equations are

$$\frac{\partial \rho}{\partial t} = C\rho\kappa \tag{4a}$$

$$\frac{\partial C}{\partial t} = -\kappa\rho e_\rho, \tag{4b}$$

where κ is the mean curvature of S and e_ρ means $e'(\rho)$. We define curvature κ as the trace of the curvature tensor with respect to the external normal. For a sphere of radius R, $\kappa = -2/R$. Equation (4a) is mass conservation. Equation (4b) is the normal component of Newton's second law. Equations (4a) and (4b) govern the evolution of the surface of the film, the normal velocity field C, and the density field ρ.

The system (4a) and (4b) is deeply nonlinear. Nonlinearity comes from several sources: curvature, interplay between velocity and density, and, most crucially, from the deforming surface. Closed form analytical solutions are few and far between even in quasistatic problems with moving surfaces that often arise in physical problems with a variational formulation [19,20].

The deformation of the domain precludes an introduction of time independent Eulerian coordinates as traditionally done in fluid mechanics. Therefore, a complete analogy with hydrodynamics—a closed system in terms of velocities and densities—is not possible. Nevertheless, a great deal of analogy may be achieved by employing the calculus of moving surfaces which has been used in quasistatic contexts [19,20].

For the classic Laplace model of surface tension (1), the system reads

$$\frac{\partial \rho}{\partial t} = C\rho\kappa, \tag{5a}$$

$$\rho\frac{\partial C}{\partial t} = \kappa\sigma. \tag{5b}$$

Equations on moving surfaces require a rule for constructing surface coordinates at all times. The presented system assumes that surface coordinates evolve according to the *normal* rule: At the initial moment, the surface coordinates are assigned arbitrarily. Subsequently, the coordinate system evolves in such a way that trajectories of constant surface coordinates are orthogonal to the surface of the fluid film. In a sense, normal coordinates are "orthogonal in time" and therefore simplify the analysis of time evolution similarly to the way Cartesian coordinates simplify spatial analysis.

The presented system focuses on the deformations of the fluid film in the normal direction and neglects the tangential components of the velocity field. The proposed equations are a simplification of the more complicated system suggested in [18,21] where the derivation was presented on the basis of the least action principle with the natural Lagrangian $L = \frac{1}{2}\int_S \rho(C^2 + V^2)dS - \int_S \rho e(\rho)dS$. The general equations read

$$\begin{aligned} \frac{\partial \rho}{\partial t} + \boldsymbol{\nabla}\cdot(\rho\mathbf{V}) &= \rho C\kappa \\ \frac{\partial C}{\partial t} + 2\mathbf{V}\cdot\boldsymbol{\nabla}C + \mathbf{V}\cdot\mathbf{B}\mathbf{V} &= -\frac{1}{\rho}\kappa p(\rho) \\ \frac{\partial \mathbf{V}}{\partial t} - \mathbf{N}(\mathbf{V}\cdot\mathbf{B}\mathbf{V}) + \mathbf{V}\cdot\boldsymbol{\nabla}\mathbf{V} - \mathbf{V}\cdot\boldsymbol{\nabla}(C\mathbf{N}) - C\boldsymbol{\nabla}C - 2C\mathbf{B}\mathbf{V} &= -\frac{1}{\rho}\boldsymbol{\nabla}p(\rho), \end{aligned} \tag{6}$$

where $p(\rho)$ is defined as

$$p(\rho) = \rho^2 e'(\rho). \tag{7}$$

The additional third vector equation governs the evolution of the tangential velocity field $\mathbf{V}$. The operator $\boldsymbol{\nabla}$ represents the surface gradient, $\mathbf{N}$ is the unit normal, and $\mathbf{B}$ is the curvature tensor (of which κ is the trace).

It can be seen that Eqs. (4a) and (4b) are formally obtained from the first two equations in (6) by setting $\mathbf{V} = 0$. Interestingly, the last equation shows that, in absence of viscosity, normal oscillations described by C will over time give rise to nonzero tangential velocities.

Properties of the equations.—Equations (4a) and (4b) satisfy mass conservation and energy conservation, while the full system of Eqs. (6) additionally conserve two-dimensional vorticity and circulation around a closed material loop. Note, that local mass conservation is evident from Eq. (4a) since change in area is proportional to mean

curvature κ (and, naturally, to C). Therefore density must change at the rate of $-C\kappa\rho$. The first equation in (6) also captures the influx of fluid due to the tangential flow.

The presented dynamic system leads to a defect in the implied equilibrium condition. The equilibrium condition is obtained by setting C to zero in Eq. (4b). The result is

$$\kappa = 0. \tag{8}$$

This is the familiar equation that characterizes surfaces of minimal area. However, this equation says nothing about the equilibrium distribution of density. Therefore, the presented dynamic equations lead to the conclusion that any density distribution can be found in equilibrium as long as the shape satisfies the zero mean curvature condition (8).

This problem can be overcome, as was suggested by Gibbs, by applying the principle of minimum energy. The first variation of the potential energy, subject to conservation of mass, is given by

$$\delta V = \int_S \left(\frac{d(\rho e(\rho))}{d\rho} - \lambda \right) \delta\rho dS, \tag{9}$$

where $\delta\rho$ is an independent variation of density and λ is the Lagrange multiplier associated with mass conservation. Equation (9) leads to the equilibrium condition

$$\frac{d(\rho e(\rho))}{d\rho} = \lambda. \tag{10}$$

In other words, unless the standard surface tension model (1) is chosen, the equilibrium distribution of ρ is uniform

$$\rho = \rho_0, \tag{11}$$

where ρ_0 is of course calculated from the total mass. For the standard surface tension model $d(\rho e(\rho))/d\rho$ is identically zero, causing the defect.

Linear analysis.—We now analyze small oscillations about stable equilibrium configurations and show that they are consistent with the existing infinitesimal models. Let ρ_0 be the equilibrium density configuration, and assume that $\partial\rho/\partial t$ and C are small. Since the equilibrium value of κ is zero, we must also assume that κ is small in the course of small oscillations. Therefore, linearized conservation of mass reads

$$\frac{\partial\rho}{\partial t} = 0. \tag{12}$$

This equation indicates that for small oscillations, density remains constant. Therefore the infinitesimal models of [13,14] are consistent with our framework in the limit of small oscillations.

The acceleration equation (4b) can be linearized by an application of the time derivative. The key identity from the calculus of moving surfaces is

$$\frac{\partial\kappa}{\partial t} = \Delta C + C\mathbf{B}{:}\mathbf{B}, \tag{13}$$

where Δ is the surface Laplacian and $\mathbf{B}{:}\mathbf{B}$ represents the trace of the matrix square of the curvature tensor $\mathbf{B}$.

For surfaces with zero mean curvature, the quantity $\mathbf{B}{:}\mathbf{B}$ equals minus twice the Gaussian curvature K. Therefore, the linearized acceleration equation reads

$$\frac{\partial^2 C}{\partial t^2} = -A_0(\Delta C - 2CK), \tag{14}$$

where $A_0 = \rho_0 e'(\rho_0)$. For the standard surface tension model, $A_0 = -\sigma/\rho_0$. For flat equilibrium configurations, $K = 0$ and infinitesimal waves are governed by the wave equation

$$\frac{\partial^2 C}{\partial t^2} = -A_0\Delta C, \tag{15}$$

consistent with [14].

Numerical computations.—Our numerics focus on Eqs. (5a) and (5b) for Laplace's equation of state (1). This system can be solved by finite differences on regular meshes. We solve the equations for one-dimensional fluid films. We do so in order to avoid the numerical artifacts associated with two-dimensional meshes for which resolution in space and time is more limited. On the other hand, one-dimensional simulations cannot be used for accurate comparisons with existing experimental data. Therefore, the main goal of this section is to demonstrate that the proposed equations hold promise for capturing certain nonlinear features of fluid film dynamics, including thickening. We are yet to attempt numerical solution of the full system (6).

We first demonstrate that the profile shape and the frequency of oscillation depend on the amplitude of the oscillations. Figure 1 shows six profiles at the moments of largest deviation from the equilibrium for initially flat [0, 1] configurations, with uniform initial density $\rho = 0.5$, initial velocity fields $C = F\sin\pi x$ with $F = 0.5, 1, 2, 3, 4$. The initial configuration was represented by a regular grid with 201 nodes. The boundary conditions are $C(0) = C(1) = 0$ for all simulations. We used MATLAB's ODE45 routine to advance in time. We observe the strong nonlinear

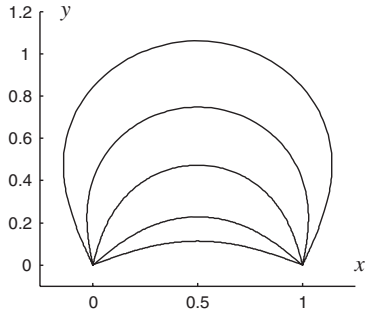

FIG. 1. Profiles at maximum deformations from equilibrium of initially flat configurations of length 1, uniform density $\rho = 0.5$, and initial velocity $C = F\sin\pi x$, where $F = 0.5, 1, 2, 3, 4$.

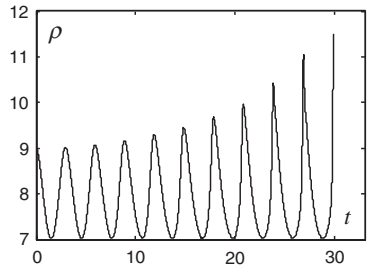

FIG. 2. Evolution of ρ at the middle point of an oscillating one-dimensional film of length 1, initially uniform density of $(x) \equiv 9$ and initial velocity profile $0.25 \sin \pi x$.

dependence of shape on the initial velocity. Although it is not indicated in the figure, the observed profiles are not periodic in time. The following paragraph speaks to this point as well.

We next illustrate the effect of thickening. For the sake of higher accuracy and greater confidence that the observed effect is not a numerical artifact, we again consider a one-dimensional film. It is initially flat, has length 1 and has uniform density of $\rho(x) \equiv 9$. The initial velocity profile is $C(x) = 0.25 \sin \pi x$. Figure 2 shows the density at the middle point $x = 0.5$ over a period of 30 nominal seconds. Figure 2 vividly demonstrates several nonlinear effects, including nonperiodicity of motion, asymmetry of motion with respect to the horizontal axis, and, finally, the growing amplitude in density oscillations. These features are consistently exhibited for different initial velocity profiles as well as varying parameters that control the numerical schemes.

The proposed equations are shift invariant. Therefore for periodic initial conditions, there exists solutions that remain periodic. Our numerical simulations indicate that these solution are dynamically stable. Therefore, periodic solutions display all of the same nonlinear effects within each period which is qualitatively consistent with available experiments [9].

Conclusions.—We have put forth a system of nonlinear equations designed to capture the nonlinear features of the dynamics of fluid films with large deformations and large variations in density, both spatial and temporal. Surprisingly, despite the fact that the proposed system purposefully disregards the tangential components of the velocity field, it leads to the growing amplitude in the oscillations of the density field. This is qualitatively consistent with available experiments [9]. Our numerical simulations exhibited further nonlinear effects such as nonperiodicity of oscillations, nonlinear dependence of shape on the initial velocity, and the emergence of traveling and reflecting density waves.

[1] D. S. Dean and R. R. Horgan, Phys. Rev. E **65**, 061603 (2002).
[2] H. Kellay and W. Goldburg, Rep. Prog. Phys. **65**, 845 (2002).
[3] O. Greffier, Y. Amarouchene, and H. Kellay, Phys. Rev. Lett. **88**, 194101 (2002).
[4] M. Rivera, P. Vorobieff, and R. E. Ecke, Phys. Rev. Lett. **81**, 1417 (1998).
[5] B. K. Martin, X. L. Wu, W. I. Goldburg, and M. A. Rutgers, Phys. Rev. Lett. **80**, 3964 (1998).
[6] E. A. van Nierop, B. Scheid, and H. A. Stone, J. Fluid Mech. **602**, 119 (2008).
[7] T. Tran, P. Chakraborty, G. Gioia, S. Steers, and W. Goldburg, Phys. Rev. Lett. **103**, 104501 (2009).
[8] D. E. Moulton and J. A. Pelesko, Phys. Rev. E **81**, 046320 (2010).
[9] M. Drenckhan, B. Dollet, S. Hutzler, and F. Elias, Philos. Mag. Lett. **88**, 669 (2008).
[10] G. Debregeas, P. Martin, and F. Brochard-Wyart, Phys. Rev. Lett. **75**, 3886 (1995).
[11] A. Boudaoud, Y. Couder, and M. B. Amar, Phys. Rev. Lett. **82**, 3847 (1999).
[12] T. Gilet and J. Bush, Phys. Rev. Lett. **102**, 014501 (2009).
[13] L. Durand, Am. J. Phys. **49**, 334 (1981).
[14] C. Isenberg, *The Science of Soap Films and Soap Bubbles* (Dover Publications, New York, 1992).
[15] J. Chomaz and M. Costa, *Thin Film Dynamics in Free Surface Flows*, CISM Courses and Lectures Vol. 391 (Springer, New York, 1998), pp. 44–99.
[16] Y. Couder, J. Chomaz, and M. Rabaud, Physica D (Amsterdam) **37**, 384 (1989).
[17] J. Serrin, *Mathematical Principles of Classical Fluid Mechanics* (Springer-Verlag, Berlin, 1959).
[18] P. Grinfeld, Stud. Appl. Math. (in press).
[19] P. Grinfeld, Phys. Rev. Lett. **87**, 095701 (2001).
[20] P. Grinfeld and H. Kojima, Phys. Rev. Lett. **91**, 105301 (2003).
[21] P. Grinfeld, J. Geom. Symm. Phys. **16**, 1 (2009).